

Case Report

Modeling the thermal performance of hybrid paraffin-air nanostructure in a heat sink: Effect of atomic ratio of Al₂O₃ nanoparticles

Wed khalid Ghanim^a, Rassol Hamed Rasheed^b, Ahmed Shawqi Sadeq^a, Mohammad N. Fares^a, Soheil Salahshour^{c,d,e}, Rozbeh Sabetvand^{f,*}

^a Chemical Engineering Department, University of Basrah, Basrah, Iraq

^b Air Conditioning Engineering Department, Faculty of Engineering, Warith Al-Anbiyaa University, Iraq

^c Faculty of Engineering and Natural Sciences, Istanbul Okan University, Istanbul, Turkey

^d Faculty of Engineering and Natural Sciences, Bahcesehir University, Istanbul, Turkey

^e Faculty of Science and Letters, Piri Reis University, Tuzla, Istanbul, Turkey

^f Department of Energy Engineering and Physics, Faculty of Condensed Matter Physics, Amirkabir University of Technology, Tehran, Iran

ARTICLE INFO

Keywords:

Thermal performance

Al₂O₃ nanoparticles

Phase change materials

Molecular dynamics simulation

ABSTRACT

This study investigates the effect of varying atomic ratios (1 %, 3 %, 6 %, and 10 %) of Al₂O₃ nanoparticles on the thermal performance of a hybrid paraffin-air nanostructure in a heat sink, using molecular dynamics simulations. The primary objective is to enhance the thermal properties of phase change materials for efficient energy storage, which is crucial for advancing thermal management systems. The purpose is to optimize nanoparticle concentration and assess how altering the atomic ratio of Al₂O₃ nanoparticles can improve thermal conductivity and heat flux within the phase change material matrix. The results demonstrate that after reaching equilibrium within 20 ns, the total energy of the atomic sample converges to -5990.70 eV, indicating stable atomic oscillations. Notably, increasing Al₂O₃ nanoparticle concentration to 3 % significantly improves the heat flux and thermal conductivity, reaching values of 354.11 W/m² and 405.42 W/m·K, respectively. The radial distribution function analysis shows a decrease in the maximum peak to 3.49 at the 3 % concentration, suggesting that a higher concentration of oxygen atoms in the material could enhance thermal performance. Furthermore, the maximum temperature within the system increases to 934.17 K at the 3 % atomic ratio. The aggregation time at this concentration is 8.11 ns, which decreases to 6.83 ns at a 10 % atomic ratio, further supporting the detrimental impact of nanoparticle aggregation. Notably, a 3 % concentration is found to be optimal for improving performance. These findings show the critical role of Al₂O₃ nanoparticles in enhancing the thermal performance of phase change material-based systems, offering valuable insights into optimal nanoparticle concentration and aggregation for effective thermal management in energy storage applications.

1. Introduction

Interest in renewable energy sources has grown significantly in recent years, as nations seek to expand their economies while meeting increasing energy demands [1]. Among various energy forms, thermal energy, particularly solar energy, has garnered attention for its potential to provide sustainable and efficient solutions [2]. A major challenge for technology experts today is developing efficient energy storage methods that facilitate the conversion into various forms as needed [3]. Energy storage plays a crucial role in balancing supply and demand, ensuring that the available energy meets consumption needs [4]. It enhances the

efficiency and reliability of energy systems while contributing to total energy conservation [5]. One promising technology for future thermal energy storage is the use of phase change materials (PCMs) [6]. PCMs have the unique ability to store heat without a significant temperature (Temp) change [7]. Heat energy transfer occurs when a material undergoes a phase change (PC), such as melting from solid to liquid or freezing from liquid to solid [8]. Heat transfer (HT) occurs during phase transitions, such as when materials change from solid to liquid or vice versa. This process enables PCMs to store and release thermal energy [9]. They are typically categorized into three groups: organic, inorganic, and eutectic materials [10]. These materials can be tailored to function across a wide range of Ts, depending on the application. Organic PCMs

* Corresponding author.

E-mail address: rozbeh.sabetvand@iaukhsh.ac.ir (R. Sabetvand).

<https://doi.org/10.1016/j.cscee.2025.101109>

Received 25 December 2024; Received in revised form 14 January 2025; Accepted 16 January 2025

Available online 20 January 2025

2666-0164/© 2025 The Authors. Published by Elsevier Ltd. This is an open access article under the CC BY license (<http://creativecommons.org/licenses/by/4.0/>).

Abbreviations

PCM	Phase change material
PC	Phase change
MD	Molecular dynamics
NP	Nanoparticles
HF	Heat Flux
TC	Thermal conductivity
T	Temperature
TP	Thermal performance
LJ	Lennard-Jones
EAM	Embedded Atom Method
Max	Maximum
AR	Atomic Ratio
HN	Hybrid nanostructure
HPAN	Hybrid paraffin-air nanostructure
HT	Heat transfer
RDF	Radial distribution function

include paraffin and non-paraffin compounds [11], are commonly used, while inorganic PCMs include hydrated salts and metal salts [6]. Enhancing PCMs by incorporating additional elements can further improve their capacity for storing and releasing thermal energy [12]. Unlike other metal oxides, Al_2O_3 offers a balance of cost-effectiveness, availability, and high thermal conductivity (TC) to density ratio, which is crucial for PC applications [13]. Additionally, the chemical stability of Al_2O_3 ensures that nanoparticles (NPs) remain inert and do not react with PCM over time, which is essential for long-term thermal energy storage [14]. Thus, Al_2O_3 -NPs are well-suited for improving TC in hybrid nanostructures (HNs), especially in systems requiring robust and efficient thermal management [15]. Heat sinks are commonly employed in the production of electronic devices to manage heat [16]. They absorb heat and transfer it to a fluid by maximizing the contact surface between the fluid and its surroundings [17]. Incorporating PCMs into heat sinks has proven to be a promising method for enhancing thermal performance (TP) [18] and improving the efficiency [19] of heat dissipation systems. Numerous studies were conducted to explore the TP of PCMs in such applications. For example, Zhao et al. [20] investigated PCs in paraffin by incorporating metal NPs through molecular dynamics (MD) simulations. Their results demonstrated a significant improvement in the TP of structure due to the addition of NPs. Khodadadi and Hosseinizadeh [21] focused on the TP of used copper NPs and observed that the base material's TC increased. Furthermore, researchers enhanced the heat release process of conventional PCMs by incorporating NPs, enabling faster phase transitions due to their smaller size and greater surface area. Song et al. [22] demonstrated that silver NPs enhanced the TP of organic PCMs. Their findings indicated that the incorporation of silver NPs not only improved heat management but also stabilized the T of PCM. Venkataraj et al. [23] discovered that the addition of Al_2O_3 -NPs to pentaerythritol significantly enhanced both thermal resistance and chemical stability. They assessed the material's performance by subjecting it to repeated heating and cooling cycles and analyzed the dispersion of nanoparticles within pentaerythritol using energy-dispersive X-ray spectroscopy (EDX). Furthermore, various concentrations of NPs were tested through thermogravimetric analysis to evaluate their effects in combination with pentaerythritol. Bergles et al. [24] examined HT in an oscillating heat pipe using MD simulations. In their research, water served as the base fluid, enhanced by adding aluminum, copper oxide, and silver NPs. The incorporation of these NPs into the base fluid resulted in increased efficiency of the HT simulation. Ameen et al. [25] found that the HT and time within the simulation box increased with the addition of NPs. Their findings indicated that incorporating NPs enhanced the TP of PCMs, resulting in

improved charging and discharging times. Sharifpur et al. [26] investigated the effect of Al_2O_3 nanoparticle volume fraction, size, and T on the TC of glycerol-based nanofluids, finding that these nanofluids significantly enhanced TC compared to the base fluid. Ghanbarpour et al. [27] studied the TC and viscosity of Al_2O_3 /water nanofluids with concentrations ranging from 3 % to 50 %. They found that both properties increased with concentration. Li et al. [28] studied the impact of adding Al_2O_3 -NPs to paraffin wax on its thermal properties. They found that TC increased by 40 % at a 0.01 % NP volume fraction. Altohamy et al. [29] investigated the effect of different volume fractions of Al_2O_3 NPs in water-based nanofluids on the thermal properties of PCMs during charging, finding that increased concentrations of Al_2O_3 -NPs significantly reduced charging time and led to more efficient HT. Samara et al. [30] investigated the effect of adding Al_2O_3 -NPs to paraffin wax (Bio-PCM) to improve TC. They found that the TC of nanofluids increased nonlinearly with the NP volume fraction. Al_2O_3 -NPs offer distinct advantages in thermal management due to their high TC and ease of incorporation into PCMs compared to many metallic NPs. Although the TC of Al_2O_3 is not as high as other metal oxides, it remains significantly higher than conventional HT fluids by two orders of magnitude, making it an effective candidate for enhancing the TP of PCMs [31,32]. These nanoparticles improve heat transfer by enhancing the flow of heat through PCM matrix, where their efficient dispersion minimizes thermal resistance. As a result, the heat transfer process is accelerated, significantly improving the TP of PCM.

Regarding the novelty of this work, the study distinguished itself from previous efforts by focusing on how varying the atomic ratio (AR) of Al_2O_3 NPs affects the TP of a hybrid paraffin-air nanostructure (HPAN) in a heat sink. While prior research explored the role of NPs in enhancing PCMs, our work offers a detailed atomic-level investigation using MD simulation, providing insights that were not easily achievable through experimental methods. MD simulation was ideal for this study due to its ability to provide atomistic-level insights [33] and reduce the need for costly experimental setups [34]. Additionally, MD simulations provided insights into various properties at the molecular level, which were crucial for understanding the efficiency of nanofluids and PCMs in thermal applications. Using MD simulations, we can obtain detailed data on atomic-scale interactions that influenced the macroscopic properties of the system, thereby enhancing our understanding of how NPs, such as Al_2O_3 , interacted with PCMs to improve TC and overall TP. This approach enabled efficient exploration of material behavior, optimizing the TP of PCMs and advancing renewable energy technologies. The study systematically examined the effects of NP concentration on key thermal properties, such as heat flux (HF), TC, RDF, and aggregation time, thereby providing optimized solutions for applications in renewable energy, electronics cooling, and thermal management.

2. Molecular dynamics simulation

LAMMPS software was used to examine the effect of the AR of Al_2O_3 -NPs on the TP of HPAN in a heat sink. LAMMPS was chosen for this study due to its powerful capabilities in simulating complex systems, including NPs and PCMs [35]. It offered accurate modeling of atomic and molecular interactions, making it ideal for studying the effects of Al_2O_3 NPs on the thermal properties of PCMs. LAMMPS was highly flexible and efficient, supporting a wide range of potential functions, time integration methods, and boundary conditions, which made it suitable for simulating various materials and their interactions at the atomic level. Additionally, LAMMPS can handle large-scale simulations, essential for accurately representing the system's behavior over extended simulation times [36]. The simulation box was set to 100 Å in all directions, with aluminum walls simulated to model the heat sink, as shown in Fig. 1. This size ensured that the system accurately represented the bulk behavior of the materials while minimizing size effects that could distort the physical properties under investigation. The selected system size was validated by confirming that the dimensions were sufficiently large to

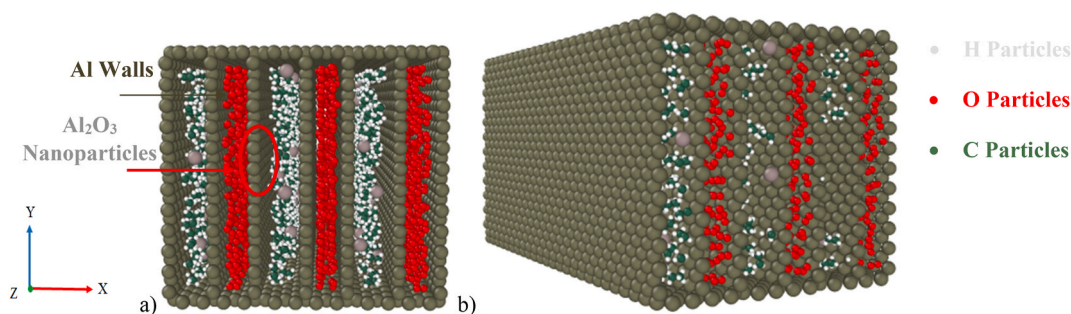


Fig. 1. A schematic of simulated HPAN from a) front and b) perspective view.

reduce the influence of boundary effects on properties of interest, such as HF. Subsequently, the paraffin structure, as the PCM, was modeled using Avogadro software [37]. Oxygen molecules (O_2 particles) were modeled using Avogadro software and packed with paraffin using PACKMOL software [38]. Next, Al_2O_3 NPs were modeled using Avogadro software, which was expanded with different atomic ratios (ARs) of 1 %, 3 %, 6 %, and 10 % using PACKMOL software (see Fig. 1). Avogadro was used to create Al_2O_3 -NPs utilizing a crystallographic file for aluminum, which was expanded to achieve the desired size and configuration of NPs. This software enabled manipulation of molecular structures, geometry adjustments, and optimization of atom arrangements, which were crucial for accurately representing Al_2O_3 -NPs in the simulation. Subsequently, PACKMOL was used to assemble the complete structure of the hybrid paraffin-NP system. PACKMOL facilitated the packing of molecules into defined spaces, allowing the effective incorporation of Al_2O_3 -NPs into the paraffin structure. This process ensured that Al_2O_3 -NPs were correctly positioned within the paraffin structure, preparing for subsequent MD simulations.

The boundary conditions were set to periodic in the Y direction and fixed in the Z and X-directions. The periodic boundary conditions applied in the Y direction simulate an infinite system along that axis, effectively mimicking a realistic HT scenario. Fixed boundary conditions in X and Z-directions represented the constraints of aluminum heat sink walls, ensuring a controlled and stable thermal environment. This configuration reflected practical applications, such as confined PCM systems in heat sinks, where the walls significantly influenced TP. After initial modeling, T was set to 300 K, and the equilibration of the structure was assessed. To evaluate this, T and total energy changes were monitored over 20 ns. In the next step, the TP of HPAN was evaluated over 30 ns using HF, RDF, TC, T profile, and aggregation time. A time step of 0.1 fs was used in the simulations. This smaller time step allowed the simulation to track faster interactions with higher precision, which was particularly important for systems with high-frequency vibrations or small NPs, such as Al_2O_3 , where atomic interactions occurred on very short timescales. It helped prevent issues like atomic overlap or divergence of the system's energy, ensuring stability throughout the simulation. The 0.1 fs time step was validated in numerous MD studies of similar systems, particularly when modeling nanofluids or materials undergoing rapid changes [39]. The embedded Atom Method (EAM) was specifically employed for aluminum atoms. EAM accurately described metallic bonding and realistically represented interactions within the aluminum components of a heat sink, ensuring high precision, particularly in capturing many-body interactions inherent in metallic systems. For other particles in the system, Lennard-Jones (LJ) potential was used to model van der Waals interactions. Eqs. (2) and (3) define the combination of LJ parameters (σ and ϵ) to represent interactions among different species. LJ potential was a reliable method for describing non-bonded interactions, particularly for organic molecules like paraffin, where dispersive forces were significant. Moreover, LJ potential was used in similar studies of PCMs and NPs, providing a solid basis for comparison with existing literature [20]. The combination of EAM for the aluminum and LJ for paraffin and NPs was selected to

ensure that metallic and non-metallic interactions were accurately modeled. Furthermore, similar studies investigating the effect of NPs in nanofluids employed EAM and LJ potential functions to model interactions within their respective systems. This further validated the appropriateness of these potential functions for the current study [40]. As shown in Fig. 1, the heat sink model used in this study included separate layers for PCM, such as paraffin, and a gas represented by oxygen molecules. This figure was created using OVITO, a powerful software tool for visualizing, analyzing, and rendering atomic structures and simulation data. It provided a clear and detailed representation of MD results [41]. This intentional design aimed to enhance the overall HT efficiency of the system. In many heat sink models, one section was designed for the flow of PCM, such as paraffin, while another section facilitated the passage of a fluid or gas, typically air [42]. This design enhanced the HT efficiency of the system by leveraging the complementary roles of PCM and air. PCM absorbed and stored a significant amount of heat during its phase transition from solid to liquid and vice versa. Meanwhile, the air or another fluid in the adjacent layer facilitated the removal of excess heat through convection. This dual approach utilized the strengths of conductive and convective heat transfer mechanisms. All MD simulation settings are reported in Table 1.

2.1. Equilibration process

The equilibration process is a fundamental step in MD simulations, ensuring that the system reaches a stable state before any properties are measured. This stage allows for the balance of kinetic and potential energies, the proper distribution of atoms, and the avoidance of artificial or unrealistic results. In the initial equilibration step, T changes in HPAN were monitored over 20 ns. The stability of T indicates that the atomic structure remained intact, with no disintegration, confirming the suitability of the potential function employed in the simulation. Moreover, the results validated that the simulation duration was sufficient, as the system reached equilibrium within 20 ns, ensuring realistic interactions and stable thermal conditions. These findings confirmed that the modeled system was well-prepared for subsequent analyses, providing a robust foundation for evaluating thermal properties. The total energy in

Table 1
Present Simulation details.

Simulation setting	value
Simulation box Dimension	$50 \times 100 \times 50 \text{ \AA}^3$
Boundary Condition	f p f
Ensemble	NVT/NVE
Initial T	300 K
Simulation duration	50 ns
Time Steps	0.1 fs
Thermostat	Nose-Hoover
Equilibration process	20 ns
Number of Atoms (Pristine Sample)	13775
Subdomain of wall	$50 \times 100 \times 50 \text{ \AA}^3$
Subdomain of paraffin/ Al_2O_3	$10 \times 100 \times 50 \text{ \AA}^3$

atomic structures, comprising kinetic and potential energies, reflected the dynamic interactions and stability of the system. This parameter was fundamental in MD simulations, providing insights into atomic interactions, movements, and overall structural stability. As a key indicator of the system's energetic state, total energy enabled a comprehensive evaluation of stability and equilibration throughout the simulation. The results illustrate the variations in total energy for HN during the simulation, demonstrating convergence to a constant value of -5990.70 eV. This steady convergence indicated that the system successfully achieved equilibrium, validating the accuracy of the applied potential function and confirming the stability of atomic configurations.

3. Radial distribution function

RDF is a critical tool for analyzing the spatial arrangement of atoms within molecular systems, providing valuable insights into their local atomic structure and behavior. In this study, RDF calculations were performed on the equilibrated atomic samples to validate the computational method employed. Specifically, RDF quantified the likelihood of finding an atom at a specific distance from a reference atom, elucidating the degree of atomic order or disorder present in the system. This metric also facilitated comparisons between simulation results and experimental or theoretical models, thereby assessing the accuracy and reliability of the MD approach.

$$J = \frac{1}{V} \left[\sum_i e_i v_i - \sum_i S_i v_i \right] = \frac{1}{V} \left[\sum_i e_i v_i - \sum_{i < j} (f_{ij} v_j) x_{ij} \right] = \frac{1}{V} \left[\sum_i e_i v_i - \frac{1}{2} \sum_{i < j} (f_{ij} \cdot (v_i + v_j)) x_{ij} \right] \quad (1)$$

ability of the MD approach. Fig. 2 illustrates carbon-carbon RDF for the paraffin structure, revealing a pronounced peak at approximately 2 \AA . This peak corresponded to the nearest-neighbor distances, indicating a well-defined local atomic arrangement. Beyond this peak, the gradual convergence of RDF values to unity reflected a transition to a homogeneous atomic distribution at larger distances, signifying that the system exhibited short-range order while maintaining long-range isotropy. These findings aligned well with experimental observations and prior theoretical studies, reinforcing the validity of the computational tools and simulation parameters used. Furthermore, the sharpness and

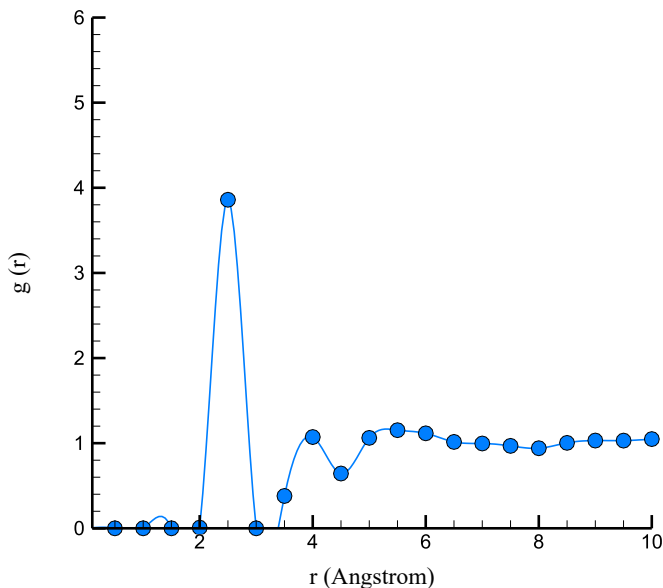


Fig. 2. Carbon-carbon RDF in paraffin structure defined after equilibration of the aluminum-paraffin-oxygen sample.

intensity of the RDF peak confirmed the stability and structural integrity of HN, which was critical for ensuring the accuracy of subsequent thermodynamic and physical analyses. The compatibility of these results with earlier research on aluminum-paraffin-oxygen systems underscored the robustness of MD methodology, particularly in capturing intricate interatomic interactions and predicting thermodynamic behavior under similar conditions [43]. This comprehensive analysis validated the reliability of the simulation framework, establishing a robust foundation for investigating more complex systems and their thermal properties.

4. Results

This section evaluated the TP of HN in the presence of different ARs of Al_2O_3 NPs. The green-Kubo method, employed to calculate thermal properties, was widely regarded as a reliable and accurate approach in MD simulations, particularly for systems with complex interactions, such as nanostructures [44]. It enabled the calculation of TC by integrating the HF autocorrelation function over time, offering insights into heat transport at the atomic level. This method was particularly suited for systems where direct measurement of TC was difficult, such as HNs involving PCMs and NPs. Green-Kubo represents in Eqs. (1) and (2):

$$K = \frac{V}{k_B T^2} \int_0^\infty (J_x(0) J_x(t)) dt = \frac{V}{3k_B T^2} \int_0^\infty (J(0) \cdot J(t)) dt \quad (2)$$

In these equations, e_i is the total particle energy of the system, S_i is the system's entropy, V represents the sample volume, k_B is Boltzmann's constant, T is the system's T , and J is the HF. Figuring out the solution to this equation helps us ascertain the extent of HF in the system. Then, it can find the TC by solving Eq. (2).

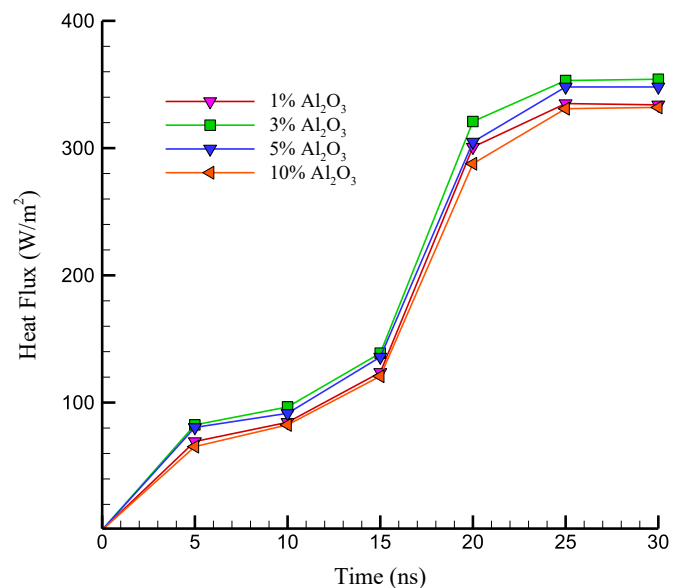


Fig. 3. Changes in HF of the HN according to the simulation time and the AR of Al_2O_3 -NPs.

HF measures the rate of heat transfer in a system and provides important insights into the system's response to heat. Incorporating Al_2O_3 NPs into HN alters the atomic distribution within the simulation box. This change in arrangement directly affects the structure of the samples and their TP. Various concentrations of Al_2O_3 -NPs, 1 %, 3 %, 6 %, and 10 %, were added to the HN. Fig. 3 illustrates the differences in HF resulting from increased concentrations of Al_2O_3 -NPs. The results indicate that increasing the concentration of Al_2O_3 -NPs up to 3 % enhanced HF. The addition of a small concentration of Al_2O_3 -NPs (up to 3 %) improved HT due to their high TC. NPs served as conductive pathways, facilitating heat transfer from hotter to cooler regions of the system. Additionally, NPs increased the surface area available for heat exchange, thereby enhancing heat transfer efficiency. However, increasing the concentration of Al_2O_3 -NPs beyond 3 % resulted in decreased HF. Higher NP concentrations raised the likelihood of aggregation, which hindered fluid flow and created thermal barriers, reducing heat transfer efficiency. The concentration of Al_2O_3 -NPs in the simulation box altered HF between 331.98 W/m^2 and 354.11 W/m^2 . This behavior of HF output in the designed system in the presence of various ratios of Al_2O_3 -based NPs detected in previous research [45]. In this research, the HF parameter increased by NP ratio increasing, but this parameter get to lesser values by NPs ratio increasing. This procedure predicted the disturbed mechanism such as NPs aggregation process decreased the thermal transfer volume (HF) in designed systems.

The following section investigated the changes in atomic structure as the concentration of Al_2O_3 NPs increases. Fig. 4 shows the variations in the maximum (Max) peak of the RDF curve over the simulation time, illustrating the effects of increasing Al_2O_3 -NP concentration. The results indicate that the maximum peak of RDF with 3 % Al_2O_3 -NPs was 3.49. As the concentration of Al_2O_3 -NPs increased further, the Max peak of the RDF curve decreased. This decrease signified changes in the spatial arrangement of atoms in the material as the concentration of Al_2O_3 -NPs increased. These alterations may affect the material's TP, including its TC and heat capacity.

The analysis of the structure's TC under varying concentrations of Al_2O_3 NPs revealed critical trends that provide insights into the behavior of nanostructured systems. Fig. 5 demonstrates the dependence of TC on Al_2O_3 -NP concentration, with a clear enhancement observed as the concentration increased up to 3 %. At this optimal concentration, TC reached a maximum value of $405.42 \text{ W/m}\cdot\text{K}$, highlighting the effective role of Al_2O_3 -NPs in facilitating thermal transport. However, beyond this

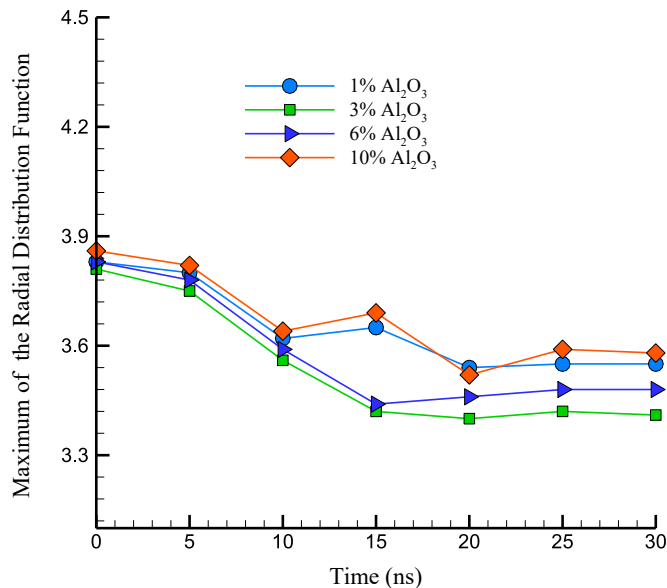


Fig. 4. The changes in the HN's Max peak of the RDF curve according to the AR of Al_2O_3 -NPs.

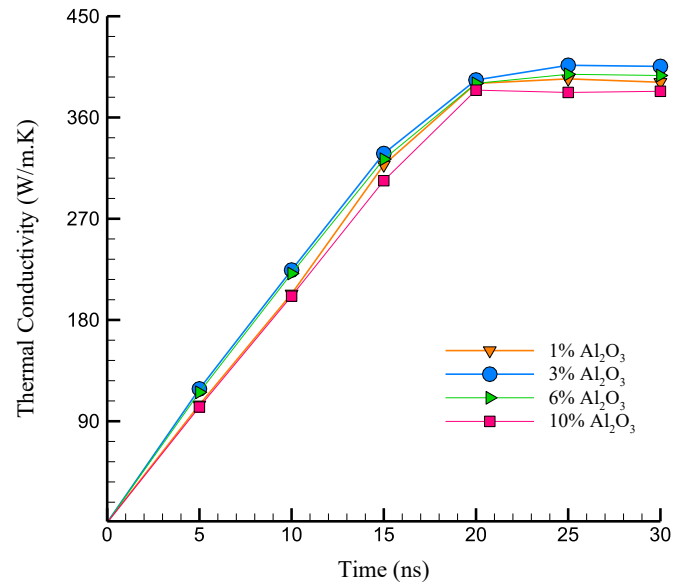


Fig. 5. The changes of the TC in the HN according to the AR of Al_2O_3 -NPs.

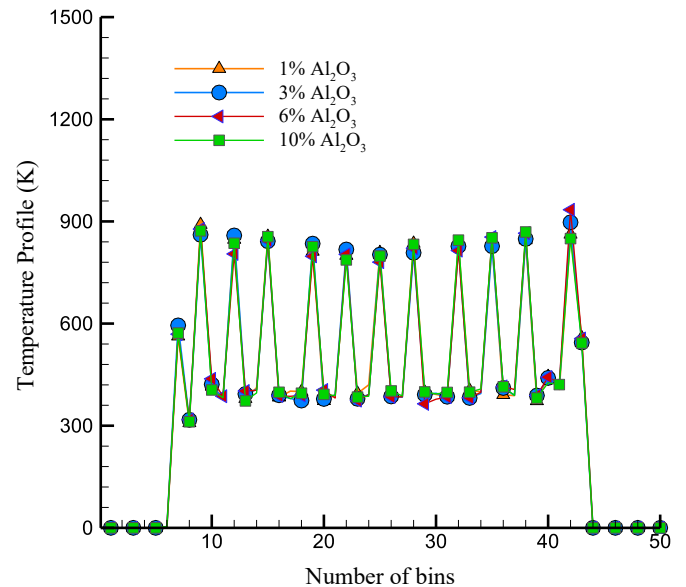


Fig. 6. T profile in the HN according to the AR of Al_2O_3 -NPs.

threshold, a decline in TC was evident as the NP concentration exceeded 3 %.

Fig. 6 illustrates how the T profile changes by increasing concentrations of Al_2O_3 NPs. The data reveal that increasing NP concentration up to 3 % led to a notable rise in Max T, reaching 934.17 K . This peak performance at 3 % was attributed to well-dispersed NPs, which formed efficient thermal pathways within the paraffin matrix. However, beyond 3 % concentration, a distinct shift in the T profile was observed. As the NP concentration increased, the aggregation propensity increased significantly. This aggregation disrupted the TC network established at lower concentrations by creating clusters of NPs that acted as thermal barriers. Consequently, T began to decline, illustrating the detrimental impact of excessive NP concentrations on the system's HT capability. At optimal concentrations, NPs were sufficiently spaced to maximize their surface area and contribute effectively to heat transfer. In contrast, at higher concentrations, reduced inter-particle distance fostered aggregation, which decreased the exposed surface area and disrupted the

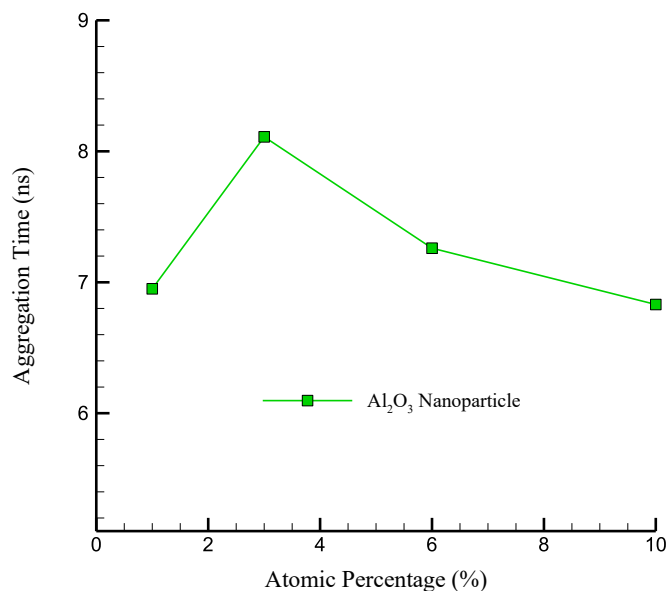


Fig. 7. Changes in aggregation time in the HN according to the AR of Al_2O_3 -NPs.

Table 2

Changes in HF, TC, RDF, T profile, and aggregation time in the HN according to the AR of Al_2O_3 -NPs.

AR of Al_2O_3 -NPs (%)	H.F (W/ m^2)	RDF (\AA)	T.C (W/ $\text{m}\cdot\text{K}$)	Max-T (K)	Aggregation time (ns)
1	323.99	3.55	391.34	890.65	6.95
3	354.11	3.41	405.42	897.32	8.11
5	348.08	3.48	397.3	934.32	7.26
10	331.98	3.58	383.29	872.35	6.83

continuity of conductive pathways. These findings underscored the critical threshold at 3 %, where the benefits of Al_2O_3 -NPs maximized without incurring the negative effects of aggregation.

Fig. 7 illustrates how the aggregation time of particles changed by increasing the concentrations of Al_2O_3 NPs. The results indicate that adding more Al_2O_3 -NPs to the system increased the aggregation time. Specifically, at a concentration of 3 %, aggregation time was approximately 8.11 ns. However, increasing the concentration to 10 % reduced the aggregation time about 6.83 ns. Numerical results are summarized in Table 2.

5. Discussion

The results indicate that adding Al_2O_3 -NPs up to 3 % enhanced HF, primarily by serving as conductive pathways. This enhancement can be attributed to the improved TC of the system with the introduction of NPs. Al_2O_3 -NPs, having a higher TC than paraffin, function as localized heat conductors within HN. The TC of aluminum was reported to be in the range of 230–300 W/ $\text{m}\cdot\text{K}$ [46,47], while paraffin's TC varied between 0.2 and 0.3 W/ $\text{m}\cdot\text{K}$ [48]. The TC of air was 0.0265 W/ $\text{m}\cdot\text{K}$ [49]. As the concentration of NPs increased, thermal energy was transferred more efficiently from hotter to cooler areas. Additionally, NPs enhanced the effective surface area for heat exchange by creating more interfaces for thermal energy absorption and transfer [12]. This enhanced heat dissipation throughout the structure, particularly at lower NP concentrations (up to 3 %), where the NPs remained well-dispersed within the paraffin matrix, facilitating smooth heat transfer. The uniform dispersion of NPs facilitated the formation of continuous heat conduction pathways, allowing thermal energy to be transferred efficiently across the material. The local movement of heat, aided by the NPs, resulted in a

more effective energy distribution throughout the system, enhancing overall thermal conductivity. Aldossary et al. [50] investigated the thermal behavior of PCMs in the presence of NPs, particularly CuO. Their results revealed that with the addition of 3 CuO NPs, HF increased significantly, which was consistent with our findings. However, when the concentration of Al_2O_3 -NPs exceeded 3 %, the likelihood of NP aggregation increased. At higher concentrations, the interparticle distance decreased, leading to the formation of NP clusters. These clusters disrupted the uniform distribution of NPs, creating local hot spots and thermal barriers that impeded heat transfer. As these aggregated regions acted as insulating zones, they blocked continuous heat flow between hot and cold areas, increasing thermal resistance. Microscopically, NP aggregation increased interfacial resistance between the NPs and the paraffin matrix and among the NPs themselves, reducing the overall thermal conductivity of the composite. These localized high-resistance regions served as barriers that hindered efficient heat transmission through the material. Consequently, heat flow began to decrease at higher NP concentrations, as observed in the simulations. This behavior highlighted the delicate balance between NP concentration and heat transfer efficiency. While NPs enhanced thermal conductivity and heat flow at lower concentrations, excessive amounts led to aggregation, undermining these benefits by introducing thermal resistance. Thus, there was a threshold concentration where the benefits of enhanced heat conduction were overshadowed by the negative effects of aggregation, highlighting the importance of maintaining an optimal NP concentration for efficient thermal management.

RDF analysis provided valuable insights into how the spatial arrangement of atoms evolved with different NP concentrations. Investigating the changes in atomic structure as the AR of Al_2O_3 NPs increases was crucial for understanding the behavior of nanostructures. At an AR of 3 %, the maximum peak of the RDF curve reached a value of 3.49, indicating a relatively well-ordered atomic structure. This suggested that NPs were well-dispersed throughout the paraffin matrix, maintaining a regular spatial arrangement that promoted efficient heat transfer and enhanced the thermal conductivity of the system. At this concentration, NPs acted as effective conductive pathways, facilitating smooth energy transfer among atoms without disrupting structural integrity. The regular atomic arrangement at this concentration facilitated the efficient transmission of kinetic energy among neighboring atoms, enhancing the TC of the system. The smooth dispersion of NPs ensured efficient energy transfer through a matrix, minimizing disruptions in atomic-level interactions that facilitated heat flow. As the AR of Al_2O_3 NPs increased beyond 3 %, the maximum peak of the RDF curve decreased. This reduction signified significant changes in the spatial arrangement of atoms, indicating the onset of NP aggregation. The decrease in the RDF peak highlighted that the atomic structure became less ordered as NPs clustered together. This clustering disrupted the regular atomic arrangement, increasing the distance between some atom pairs and reducing the overall coherence of the system. The aggregation of NPs resulted in regions where the atomic structure became less cohesive, leading to a reduction in effective atomic interactions. This clustering disrupted previously efficient pathways for thermal energy transfer, as energy transfer among atoms in these regions became less effective due to increased atomic separation and the formation of thermal barriers [51]. These barriers increased thermal resistance, impeding heat movement through the material. When NPs cluster, they create isolated regions where energy is trapped and cannot be efficiently transferred to neighboring atoms. These regions introduced significant thermal resistance, limiting overall heat flow within the material. This behavior was particularly evident at higher NP concentrations, where NP aggregation became more pronounced, leading to increased thermal resistance that outweighs the benefits of additional NPs. The loss of atomic order, indicated by the decrease in the RDF peak, correlated with a decline in TC and heat capacity. Specifically, NP aggregation reduced available surface area for effective heat transfer, undermining the benefits provided by NPs at lower concentrations. The reduced atomic order

and increased NP aggregation led to fewer interfaces for effective heat transfer between the paraffin matrix and NPs, significantly diminishing heat conduction efficiency. As NP aggregation progressed, effective thermal pathways became fragmented, decreasing the overall heat transfer rate and, consequently, the TC of the system.

In LAMMPS, the T profile referred to the variation of T across different regions of the system, providing insight into how heat was distributed within the material during simulation. This profile was crucial for understanding the thermal properties of the system, as it highlighted the transfer and diffusion of thermal energy across the modeled space. T profile was typically generated by calculating the T of particles or atoms within specific regions, known as 'bins,' within the MD simulation box. These bins allowed for spatially resolved analysis of T distribution, enhancing our understanding of thermal behaviors in different components of system. T profile was calculated by considering the center-of-mass velocity of atoms within each bin, and this data was used to obtain the overall T distribution [52]. The optimal dispersion at 3 % concentration resulted in the system's highest thermal efficiency and maximum observed T. In this state, well-dispersed NPs facilitated heat movement and played a crucial role in maintaining thermal stability by promoting a more uniform T distribution across the material. However, as the concentration of Al₂O₃ NPs increased beyond 3 %, NP aggregation occurred due to their proximity. This aggregation formed clusters that disrupted previously efficient thermal pathways by creating thermal barriers within the material. Instead of aiding heat transfer, the aggregated NPs formed isolated pockets that hindered conduction, leading to a reduction in the overall thermal efficiency of the system. Consequently, the system's ability to heat transfer diminished and the total T decreased, illustrating the negative impact of excessive NP concentration on heat transfer performance. This behavior underscored the importance of maintaining an optimal concentration of NPs in the composite material. The observed trend in this study revealed that as the concentration of Al₂O₃ NPs increased, aggregation time notably decreased, underscoring the critical role of particle interactions and dispersion in determining the system's thermal and structural behavior. At an optimal NP concentration of 3 %, the aggregation time was approximately 8.11 ns, indicating that the particles remained well-dispersed for a longer duration. This extended aggregation time reflected the stability of dispersion at this concentration, where inter-particle distances were sufficient to minimize attractive forces, such as van der Waals interactions, that drive clustering. However, as the concentration of Al₂O₃ NPs increased beyond 3 %, aggregation time significantly decreased, reaching 6.83 ns at a 10 % concentration. This reduction can be attributed to shorter inter-particle distances at higher NP concentrations, which increase the frequency and intensity of particle collisions. The closer proximity of NPs fosters stronger inter-particle interactions, leading to a more rapid onset of aggregation. Physically, this shift can be understood as a competition between the thermal motion of particles, promoting dispersion, and the attractive forces driving aggregation. At higher concentrations, the attractive forces dominate, overwhelming the stabilizing effects of thermal motion and leading to faster cluster formation. The implications of this behavior are significant for the thermal management properties of the composite. At lower NP concentrations, the extended aggregation time allowed NPs to remain dispersed, maintaining a larger effective surface area for thermal exchange and forming a continuous network of conductive pathways. This distribution facilitates efficient heat transfer, optimizing the system's thermal performance. Conversely, the rapid aggregation observed at higher NP concentrations disrupted this network, as clustered particles reduced effective surface area and acted as localized thermal barriers. These clusters hindered the uniform dissipation of heat, resulting in decreased TC and compromised thermal efficiency. From a materials design perspective, these findings emphasized the importance of optimizing NP concentration to balance dispersion and aggregation dynamics. While a higher NP concentration might intuitively seem advantageous for improving thermal properties, the

accompanying increase in aggregation rate undermines these benefits. This underscored the need to carefully optimize NP concentration to maximize the performance of NP-based composites in thermal applications. Fine-tuning this balance was essential for ensuring the composite's continued effectiveness in efficiently managing heat transfer. At an AR of 3 %, particle distribution and T profile were optimal, resulting in Max thermal efficiency. In contrast, higher concentrations resulted in rapid aggregation, diminishing the system's HT capabilities.

6. Conclusion

This study utilized computer models and techniques to examine changes in atomic structures and T within a unique heat sink made of paraffin as a PCM and air. The study was divided into two primary segments. The first segment focused on ensuring the proper distribution of atomic samples for equilibration. The second segment involved analyzing the T profile of samples over time. The main results can be categorized as follows.

- The simulated samples reached T = 300K, and it was estimated that the atomic samples reached equilibrium within 20 ns.
- After a duration of 20 ns, the atomic sample's total energy reached -5990.70 eV. This indicated the convergence of atomic oscillations to a certain value at the end of the equilibration stage.

After observing the equilibrium in the atomic samples, the TP of structures was investigated, and the following results were obtained after 30 ns.

- Increasing the concentration of Al₂O₃ NPs to 3 % enhanced HF in HPAN. However, further increases in NP concentration led to a decrease in HF. Higher NP concentrations heightened the likelihood of aggregation, which can obstruct fluid flow and create thermal barriers, thereby reducing heat transfer efficiency.
- Increasing the concentration of Al₂O₃ NPs to 3 % resulted in a decrease in the maximum peak of RDF to 3.49. However, as the concentration of Al₂O₃ NPs increased further, the higher concentration of oxygen atoms in the material could affect its thermal properties.
- TC increased to 405.42 W/m·K when the AR of Al₂O₃-NPs increased to 3 %. But, with further increase of these Al₂O₃-NPs, TC decreased.
- Increasing the concentration of Al₂O₃-NPs to 3 % increased the maximum T to 934.17 K. However, at higher concentrations of Al₂O₃-NPs, the likelihood of particle aggregation increased, which may reduce their effectiveness in enhancing TC.

The duration of aggregation time at a concentration of 3 % Al₂O₃ NPs was estimated to be 8.11 ns. With an increase to 10 % Al₂O₃ NPs, this duration decreased to 6.83 ns. At higher concentrations, the likelihood of particle aggregation increases.

7. Future perspectives

This study provided detailed insights into the TP of HPANs, revealing how the concentration of Al₂O₃ NPs influenced HT efficiency. Building on these findings, future research should explore the effects of other NP types, such as CuO, ZnO, or composite NPs that combine metallic and ceramic properties, to identify the most effective configurations for enhancing TC. Investigating NP shapes, surface functionalization, and synergistic effects within PCM matrices could also yield a more comprehensive understanding of TP optimization. Long-term stability testing under varying thermal cycles and operational conditions, such as high-T fluctuations or continuous phase-change operations, should be conducted to ensure the durability and reliability of PCM-NP systems. Addressing real-world challenges, such as NP aggregation over time and chemical compatibility with surrounding materials, was essential.

Finally, integrating optimized hybrid structures into practical thermal management systems, such as heat sinks for electronic devices or energy storage units, will require examining scalability, manufacturing feasibility, and cost-efficiency. Advanced experimental and simulation techniques can further explore how PCM-NP systems perform in dynamic environments, ensuring that the insights from this study translate into effective applications for industrial and commercial thermal management.

CRediT authorship contribution statement

Wed khalid Ghanim: Writing – review & editing, Conceptualization, Data curation, Formal analysis, Supervision, Investigation, Writing – original draft. **Rassol Hamed Rasheed:** Writing – review & editing, Conceptualization, Data curation, Formal analysis, Supervision, Investigation, Writing – original draft. **Ahmed Shawqi Sadeq:** Writing –

review & editing, Conceptualization, Data curation, Formal analysis, Supervision, Investigation, Writing – original draft. **Mohammad N. Fares:** Writing – review & editing, Conceptualization, Data curation, Formal analysis, Supervision, Investigation, Writing – original draft. **Soheil Salahshour:** Writing – review & editing, Conceptualization, Data curation, Formal analysis, Supervision, Investigation, Writing – original draft. **Rozbeh Sabetvand:** Writing – review & editing, Conceptualization, Data curation, Formal analysis, Supervision, Investigation, Writing – original draft.

Declaration of competing interest

The authors declare that they have no known competing financial interests or personal relationships that could have appeared to influence the work reported in this paper.

Appendix A. Supplementary data

Supplementary data to this article can be found online at <https://doi.org/10.1016/j.cscee.2025.101109>.

Appendix

A. MD Simulation

In investigating the TP of HPAN in a heat sink, MD simulation is a valuable tool for studying the system's atomic behavior. It enables a detailed examination of how different NP ARs affect thermal resistance, TC, and aggregation kinetics. The advantages of MD simulation, such as atomistic detail, flexibility, and predictive capabilities, make it suitable for studying complex materials and microstructures, providing valuable insights for further research and development. Potential functions are mathematical models used in MD simulation to describe interactions between atoms and molecules. They are essential for accurately predicting material behavior and simulating properties. The choice of potential function depends on the specific material and the required accuracy, making it a crucial consideration in MD simulation. This study employed a combination of LJ and EAM potentials to calculate particle energy. The form of LJ function is as follows [53]:

$$U_{LJ} = 4\epsilon \left[\left(\frac{\sigma}{r} \right)^{12} - \left(\frac{\sigma}{r} \right)^6 \right] \quad r < r_c \quad (\text{a-1})$$

The potential well depth is represented by ϵ , while σ denotes the distance at which the potential function became zero. It also measured the distance among particles, and r_c sets Max allowed radius for calculations. Table a-1 shows the information about LJ potential function for the particles in the MD simulations. Using this information and Eqs. (a-2) and (a-3), we can find the values of σ and ϵ for each particle interaction [54,55].

Table a-1. LJ potential function parameters are used in molecular dynamic simulation [54].

Particles	σ (Å)	ϵ (kcal/mol)
C	3.851	0.105
H	2.886	0.044
Al	4.499	0.505
O	3.50	0.06

$$\epsilon_{ij} = \sqrt{\epsilon_i \epsilon_j} \quad (\text{a-2})$$

$\sigma_{ij} = \frac{\sigma_i + \sigma_j}{2}$ (a-3) EAM non-bonding potential function is to show how metal particles in heat sink walls interact. It can express using Eq. (a-4) [56]:

$U_i = F_\alpha \left(\sum_{i \neq j} \rho_\beta(r_{ij}) \right) + \frac{1}{2} \sum_{i \neq j} \phi_{\alpha\beta}(r_{ij})$ (a-4) F_α is a constant value in the range of 0–1 within this equation. The density of atomic charges causes ρ_β and $\phi_{\alpha\beta}$ is caused by the presence of particles in the simulation box. In statistical mechanics, the RDF in a particle system explains how the density changes as a function of distance among the particles. The RDF of structures can be calculated using Eq. (a-5) [57]:

$$g_i(r) dr = \frac{1}{N} \sum_{i=1}^N g_i(r) dr \quad (\text{a-5})$$

In Eq. (a-5), $g(r)$ is RDF, N is the number of particles, and r is the distance among particles. A flowchart illustrating the current simulation process is provided in Fig. a-1.

Data availability

No data was used for the research described in the article.

References

- [1] S.K. Pathak, V. Tyagi, K. Chopra, B. Kalidasan, A. Pandey, V. Goel, A. Saxena, Z. Ma, Energy, exergy, economic and environmental analyses of solar air heating systems with and without thermal energy storage for sustainable development: a systematic review, *J. Energy Storage* 59 (2023) 106521.
- [2] S. Zhang, P. Octoño, J.J. Klemesš, P. Michorczyk, K. Pieliuchowska, K. Pieliuchowski, Renewable energy systems for building heating, cooling and electricity production with thermal energy storage, *Renew. Sustain. Energy Rev.* 165 (2022) 112560.
- [3] A.Z.A. Shaqsi, K. Sopian, A. Al-Hinai, Review of energy storage services, applications, limitations, and benefits, *Energy Rep.* 6 (2020) 288–306.
- [4] H.P. Garg, S.C. Mullick, V.K. Bhargava, *Solar Thermal Energy Storage*, Springer Science & Business Media, 2012.
- [5] C. Veerakumar, A. Sreekumar, Energy conservation potential through thermal energy storage medium in Buildings. Sustainability through Energy-Efficient Buildings, CRC Press, 2018, pp. 131–149.
- [6] A. Sharma, V.V. Tyagi, C.R. Chen, D. Buddhi, Review on thermal energy storage with phase change materials and applications, *Renewable and Sustainable energy reviews* 13 (2) (2009) 318–345.
- [7] Y. Liu, R. Zheng, J. Li, High latent heat phase change materials (PCMs) with low melting temperature for thermal management and storage of electronic devices and power batteries: critical review, *Renew. Sustain. Energy Rev.* 168 (2022) 112783.
- [8] K. Pillai, B. Brinkworth, The storage of low grade thermal energy using phase change materials, *Appl. Energy* 2 (3) (1976) 205–216.
- [9] A. Abhat, Low temperature latent heat thermal energy storage: heat storage materials, *Sol. Energy* 30 (4) (1983) 313–332.
- [10] P. Singh, R. Sharma, A. Ansu, R. Goyal, A. Sari, V. Tyagi, A comprehensive review on development of eutectic organic phase change materials and their composites for low and medium range thermal energy storage applications, *Sol. Energy Mater. Sol. Cell.* 223 (2021) 110955.
- [11] M.K. Rathod, J. Banerjee, Thermal stability of phase change materials used in latent heat energy storage systems: a review, *Renewable and sustainable energy reviews* 18 (2013) 246–258.
- [12] S.L. Tariq, H.M. Ali, M.A. Akram, M.M. Janjua, M. Ahmadlouydarab, Nanoparticles enhanced phase change materials (NePCMs)-A recent review, *Appl. Therm. Eng.* 176 (2020) 115305.
- [13] M. Raja, R. Vijayan, P. Dineshkumar, M. Venkatesan, Review on nanofluids characterization, heat transfer characteristics and applications, *Renewable and sustainable energy reviews* 64 (2016) 163–173.
- [14] K. Suganthi, a.S. Rajan, Metal oxide nanofluids: review of formulation, thermo-physical properties, mechanisms, and heat transfer performance, *Renew. Sustain. Energy Rev.* 76 (2017) 226–255.
- [15] E. Jitheesh, M. Joseph, V. Sajith, Comparison of metal oxide and composite phase change material based nanofluids as coolants in mini channel heat sink, *Int. Commun. Heat Mass Tran.* 127 (2021) 105541.
- [16] Q. Zhang, Z. Feng, J. Zhang, F. Guo, S. Huang, Z. Li, Design of a mini-channel heat sink for high-heat-flux electronic devices, *Appl. Therm. Eng.* 216 (2022) 119053.
- [17] I. Zahid, M. Farooq, M. Farhan, M. Usman, A. Qamar, M. Imran, M.A. Alqahtani, S. Anwar, M. Sultan, M.Y. Javaid, Thermal performance analysis of various heat sinks based on alumina NePCM for passive cooling of electronic components: an experimental study, *Energies* 15 (22) (2022) 8416.
- [18] K.S. Gopalan, V. Swaran, Numerical investigation of thermal performance of PCM based heat sink using structured porous media as thermal conductivity enhancers, *Int. J. Therm. Sci.* 104 (2016) 266–280.
- [19] M.Y. Tharwan, H.M. Hadidi, Experimental investigation on the thermal performance of a heat sink filled with PCM, *Alex. Eng. J.* 61 (9) (2022) 7045–7054.
- [20] C. Zhao, Y. Tao, Y. Yu, Molecular dynamics simulation of nanoparticle effect on melting enthalpy of paraffin phase change material, *Int. J. Heat Mass Tran.* 150 (2020) 119382.
- [21] J. Khodadadi, S. Hosseinzadeh, Nanoparticle-enhanced phase change materials (NEPCM) with great potential for improved thermal energy storage, *Int. Commun. Heat Mass Tran.* 34 (5) (2007) 534–543.
- [22] Q. Song, Y. Li, J. Xing, J. Hu, Y. Marcus, Thermal stability of composite phase change material microcapsules incorporated with silver nano-particles, *Polymer* 48 (11) (2007) 3317–3323.
- [23] K. Venkitaraj, S. Suresh, B. Praveen, A. Venugopal, S.C. Nair, Pentaerythritol with alumina nano additives for thermal energy storage applications, *J. Energy Storage* 13 (2017) 359–377.
- [24] A. Bergles, M. Chyu, in: *Characteristics of Nucleate Pool Boiling from Porous Metallic Coatings*, 1982.
- [25] M.M. Ameen, K. Prabhul, G. Sivakumar, P.P. Abraham, U. Jayadeep, C. Sobhan, Molecular dynamics modeling of latent heat enhancement in nanofluids, *Int. J. Thermophys.* 31 (2010) 1131–1144.
- [26] M. Sharifpur, N. Tshimanga, J.P. Meyer, O. Manca, Experimental investigation and model development for thermal conductivity of α -Al₂O₃-glycerol nanofluids, *Int. Commun. Heat Mass Tran.* 85 (2017) 12–22.
- [27] M. Ghanbarpour, E.B. Haghigi, R. Khodabandeh, Thermal properties and rheological behavior of water based Al₂O₃ nanofluid as a heat transfer fluid, *Exp. Therm. Fluid Sci.* 53 (2014) 227–235.
- [28] D. Li, Z. Wang, Y. Wu, C. Liu, M. Arici, Experimental investigation on thermal properties of Al₂O₃ nanoparticles dispersed paraffin for thermal energy storage applications, *Energy Sources, Part A Recovery, Util. Environ. Eff.* 46 (1) (2024) 8190–8200.
- [29] A.A. Altohamy, M. Abd Rabbo, R. Sakr, A.A. Attia, Effect of water based Al₂O₃ nanoparticle PCM on cool storage performance, *Appl. Therm. Eng.* 84 (2015) 331–338.
- [30] H. Samara, M. Hamdan, O. Al-Oran, Effect of Al₂O₃ nanoparticles addition on the thermal characteristics of paraffin wax, *International Journal of Thermofluids* 22 (2024) 100623.
- [31] S. Mallakpour, M. Dinari, Enhancement in thermal properties of poly (vinyl alcohol) nanocomposites reinforced with Al₂O₃ nanoparticles, *J. Reinforc. Plast. Compos.* 32 (4) (2013) 217–224.
- [32] J. Xu, K. Bandyopadhyay, D. Jung, Experimental investigation on the correlation between nano-fluid characteristics and thermal properties of Al₂O₃ nano-particles dispersed in ethylene glycol–water mixture, *Int. J. Heat Mass Tran.* 94 (2016) 262–268.
- [33] A. Aman, in: *Silico Study on Inclusion Complex of Sorafenib and Regorafenib with Modified Cyclodextrins*, 2022.
- [34] S. Barbhuiya, B.B. Das, Molecular dynamics simulation in concrete research: a systematic review of techniques, models and future directions, *J. Build. Eng.* (2023) 107267.
- [35] C. Zhao, Y. Tao, Y. Yu, Thermal conductivity enhancement of phase change material with charged nanoparticle: a molecular dynamics simulation, *Energy* 242 (2022) 123033.
- [36] Y. Peng, C. Knight, P. Blood, L. Crosby, and G. A. Voth, "Extending Parallel Scalability of LAMMPS and Multiscale Reactive Molecular Simulations." pp. 1-7.
- [37] M.D. Hanwell, D.E. Curtis, D.C. Lonie, T. Vandermeersch, E. Zurek, G.R. Hutchison, Avogadro: an advanced semantic chemical editor, visualization, and analysis platform, *J. Cheminf.* 4 (2012) 1–17.
- [38] L. Martínez, R. Andrade, E.G. Birgin, J.M. Martínez, PACKMOL: a package for building initial configurations for molecular dynamics simulations, *J. Comput. Chem.* 30 (13) (2009) 2157–2164.
- [39] H. Zerradi, H. Loulifat, Numerical simulation of thermal conductivity of aqueous nanofluids containing graphene nanosheets using molecular dynamics simulation, *MOJ Appl Bion Biomech* 2 (6) (2018) 313–322.
- [40] Y. Wang, J. Zheng, G.F. Smaism, D. Toghraie, RETRACTED: Molecular Dynamics Simulation of Phase Transition Procedure of Water-Based Nanofluid Flow Containing CuO Nanoparticles, Elsevier, 2022.
- [41] A. Stukowski, Visualization and analysis of atomistic simulation data with OVITO—the Open Visualization Tool, *Model. Simulat. Mater. Sci. Eng.* 18 (1) (2009) 015012.
- [42] M. Jaworski, and R. Domański, "A Novel Design of Heat Sink with PCM for Electronics Cooling."
- [43] J.S. Jayan, S. Appukuttan, R. Wilson, K. Joseph, G. George, K. Oksman, An introduction to fiber reinforced composite materials. *Fiber Reinforced Composites*, Elsevier, 2021, pp. 1–24.
- [44] M.S. Green, Markoff random processes and the statistical mechanics of time-dependent phenomena. II. Irreversible processes in fluids, *The Journal of chemical physics* 22 (3) (1954) 398–413.
- [45] H. Moghadasi, N. Malekian, H. Saffari, A. Mirza Gheithaghy, G.Q. Zhang, Recent advances in the critical heat flux amelioration of pool boiling surfaces using metal oxide nanoparticle deposition, *Energies* 13 (15) (2020) 4026.
- [46] A. Zhang, Y. Li, Thermal conductivity of aluminum alloys—a review, *Materials* 16 (8) (2023) 2972.
- [47] E. Kaschnitz, W. Funk, T. Pabel, Electrical resistivity measured by millisecond pulse-heating in comparison to thermal conductivity of the aluminium alloy Al-7Si-0.3 Mg at elevated temperature, *High Temp Press* 43 (2014) 175–191.
- [48] Z. Wang, Z. Zhang, L. Jia, L. Yang, Paraffin and paraffin/aluminum foam composite phase change material heat storage experimental study based on thermal management of Li-ion battery, *Appl. Therm. Eng.* 78 (2015) 428–436.
- [49] Y. Yao, H. Wu, Z. Liu, Pore scale investigation of heat conduction of high porosity open-cell metal foam/paraffin composite, *J. Heat Tran.* 139 (9) (2017) 091302.
- [50] A.S. Aldossary, N. Sulaiman, PCM examine of Silica/Decane nanostructure in the presence of copper oxide nanoparticles to improve the solar energy capacity of glass in the solar collectors via MD approach, *Eng. Anal. Bound. Elem.* 145 (2022) 72–82.
- [51] J. Khodadadi, L. Fan, H. Babaei, Thermal conductivity enhancement of nanostructure-based colloidal suspensions utilized as phase change materials for thermal energy storage: a review, *Renew. Sustain. Energy Rev.* 24 (2013) 418–444.
- [52] https://docs.lammps.org/compute_temp_profile.html.
- [53] J.E. Lennard-Jones, Cohesion, *Proc. Phys. Soc.* 43 (5) (1931) 461.
- [54] A.K. Rappé, C.J. Casewit, K. Colwell, W.A. Goddard III, W.M. Skiff, UFF, a full periodic table force field for molecular mechanics and molecular dynamics simulations, *J. Am. Chem. Soc.* 114 (25) (1992) 10024–10035.
- [55] S.L. Mayo, B.D. Olafson, W.A. Goddard, DREIDING: a generic force field for molecular simulations, *Journal of Physical Chemistry* 94 (26) (1990) 8897–8909.
- [56] M.S. Daw, S.M. Foiles, M.I. Baskes, The embedded-atom method: a review of theory and applications, *Mater. Sci. Rep.* 9 (7–8) (1993) 251–310.
- [57] H. Toubaa, G.A. Mansoori, An analytic expression for the first shell of the radial distribution function, *Int. J. Thermophys.* 18 (1997) 1217–1235.